Determining the shear-rate of shear-thinning fluids at the surface with an ultrasonic waveguide viscometer

by

Sabine van Dijk

to obtain the degree Bachelor of Science
at Delft University of Technology,
to be defended publicly on December 1st, 2021.

Student number:	4965469	
Project duration:	30th of August, 2021 - 1st of December, 2021	
Thesis committee:	Dr.ir. Martin Rohde,	TU Delft, supervisor
	Dr.ir. Danny Lathouwers,	TU Delft

Abstract

On the road to lower the carbon emission, nuclear energy plays a significant role. The Molten Salt Fast Reactor (MSFR) is a reactor investigated by the Reactor institute Delft in order to make it a safe and efficient energy source for the future. Properties of the fuel salt in the MSFR, such as density and rheology need to be known in order to predict the flow behaviour of the fluid. Because of the extreme circumstances in the reactor, like the high temperature and radioactivity of the molten salt, an ultrasonic waveguide is used to determine the rheological parameters of the molten salt.

In this thesis, the shear-rate on the boundary, of a wave generated by a ultrasonic waveguide viscometer is investigated. This investigation is done on the following shear thinning fluids: blood, ketchup and soybean oil. When more is known about this shear-rate for these non-Newtonian fluids this can be used to find the rheological parameters of the fluid.
As to determine the relation for the shear-rate, a dimension analysis is performed. This dimension analysis gives a relation for the shear-rate to dimensionless parameters, a constant pre-factor k and a constant power δ. This relation is tested in a computer simulation of the waveguide experiment. The value for B and ω of the shear-wave generated by the waveguide are altered, and the simulation then produces the corresponding shear-rate in the fluid. Then, the obtained shear-rate is plotted over the dimensionless parameter. After this, the pre-factor k and the power of the dimensionless parameter δ can be determined, using least squares fitting of the data to the relation from the dimensional analysis.

When the relation was tested for different values of B, the fitted δ and k were almost the same for the ketchup and soybean oil. The fitted δ and k for blood were different. This means there is probably a second dimensionless parameter that needs to be taken into account. When the relation was tested for different values of ω the values for δ were in the same range for the three fluids. The fitted k on the other hand differed too much between the fluids to be an error in the measurement. Both varying B and varying ω gives results that indicate a missing dimensionless parameter.

Further research can be done on finding the parameters the missing dimensionless parameter depends on. After this dimensionless parameter is found its power and the pre-factor k should be determined in order to find the relation for the shear-rate.

Table of contents

1. Introduction

As the demand for energy keeps increasing, and the battle against global warming continues, non-fossil energy sources are needed. Nuclear energy generation is very promising as it can produce a lot of energy while producing almost no waste, no greenhouse gasses and it does not rely on inconsistent energy sources like the sun or the wind. However, due to nuclear disasters like Chernobyl (1986) and Fukushima (2011) nuclear energy is prone to more criticism about safety of the environment and public health. The Generation IV International Forum (GIF) is set up with the aim to develop sustainable, safe and efficient nuclear reactors[1]. The Molten Salt Fast Reactor (MSFR) is one of those generation IV reactors. The SAMOSAFER (Severe Accident Modelling and Safety Assessment for Fluid-fuel Energy Reactors) project aims to ensure that the MSFR can comply with all safety measurements in 30 years time [2].

In order to comply with the safety measurements research needs to be performed on the fluid behaviour. Properties of the fuel salt that determine the fluid behavior such as density and rheology need to be studied. However, because of the severe circumstances in the reactor, like the high temperature and radioactivity of the fluid, these properties are hard to measure. For measuring the rheological properties an ultrasonic waveguide is used. This research studies the shear-rate of shear-thinning fluids such that this ultrasonic waveguide will eventually be able to measure the rheological constants for power law fluids in the MSFR.

1.1. Molten Salt Fast Reactor

The Molten Salt Fast Reactor (MSFR) is the only generation IV reactor with a liquid salt carrying the fuel[1]. The molten salt is inside a cilindrical vessel at an operating temperature of 750 C and kept at ambient pressure[2]. The advantage of a liquid fuel over a solid fuel is that it functions as a transporter and a coolant at the same time. To avoid overheating there is also a freeze plug inside the MSFR. If the salt is too hot, the freeze plug will melt and the salt will be stored in separate containers under the reactor core. This makes the reactor inherently safe. In figure 1, the core of the MSFR, containing the molten salt fuel is displayed.

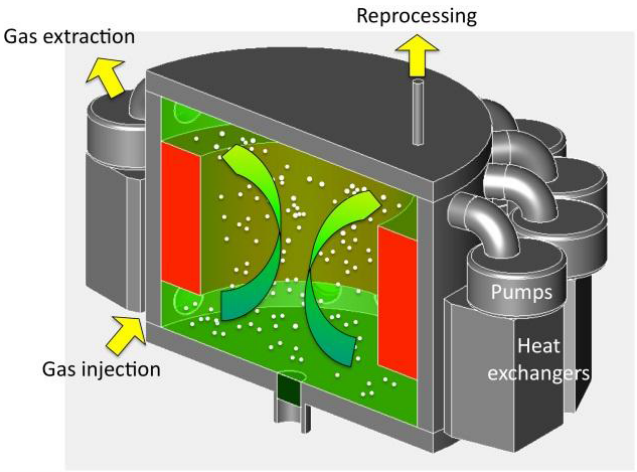

Figure 1: Schematic representation of the MSFR core. In green is the molten salt. The red parts form a cilinder of thorium, the breeding blanket. [2]

The fuel salt in the MSFR is a mixture of 232Th, 233U and Li fluorides.[3] Thorium-232 is the base for the fuel. Thorium-232 is not fissile on itself but when it captures a neutron it can transform into the fissile uranium-233. Because a neutron is needed to transform the thorium in the fissile uranium, the fluid must contain a large amount of neutrons. This way the reactor is as efficient as possible. The SAMOSAFER project studies the properties of this fluid to be able to make the MSFR comply with the safety regulations.

1.2. Previous research

The setup that is used for measuring the flow of the molten salt fuel in the MSFR is investigated experimentally by Rook [4] for Newtonian fluids. Rook succeeded in measuring the viscosity at room temperature for low viscous Newtonian fluids. Since there exists an analytical solution to the velocity profile for a Newtonian fluid this could be used to find the shear-rate. This shear-rate could then be used to find the viscosity of the Newtonian fluid. For non-Newtonian fluids, there is no analytical solution to the velocity profile. Hence, the shear-rate cannot be derived from this. As the fuel of the MSFR is likely to be a non-Newtonian power law fluid, this raises a difficulty in finding the rheological properties of the molten salt fluid using Rook's method.

Borstlap and Schuringa followed this research with their own researches [5],[6]. Their researches mimicked the experiment of Rook in a computer simulation and used this simulation to obtain the rheological properties for non-Newtonian fluids.

The shear-rate they used to obtain these rheological properties was first proposed by Rohde [7] based on results from previous research by Ai and Vafai [8]. This shear-rate gave good solutions in finding the flow index, n, but was less successful in finding the consistency rate, K. In addition to this shear-rate Schuringa proposed two other possible solutions for the shear-rate which were proved to be more successful in finding the consistency rate, K. Yet, significant deviations from the theoretical values were found.

1.3. Thesis outline

The main goal of this research is to find a shear-rate that can solve for the rheological properties K and n in the ultrasonic waveguide setup. As there is no analytical solution to the shear-rate and the earlier proposed shear-rates were on its own only good for calculating one of the two rheological constants, a good solution to the shear-rate for non Newtonian fluids is still needed. This formulates the research question:

- What is the relation for the shear-rate of shear-thinning fluids in the ultrasonic waveguide setup?

This relation is firstly determined with a dimension analysis. The equation from the dimension analysis has an unknown prefactor, k and an unknown power for the dimensionless parameter, δ. To find these constants a computer simulation is executed to find the shear-rate for different values of the dimensionless parameter. The used computer simulation mimics the ultrasonic waveguide setup and is based on the simulation code used by Borstlap and Schuringa [5][6]. The outcome for the shear-rate from these simulations is then plotted over the dimensionless parameter. The data of this plot is fitted to the equation found in the dimension analysis to find

the constants k and δ and ultimately describing the shear-rate of shear-thinning fluids in the ultrasonic waveguide setup.

In chapter 2 the theoretical background of the experiment is explained. After this, chapter 3 focuses on explaining the experiment that is performed to obtain the results. Chapter 4 presents and discusses the obtained results. Concluding with chapter 5 wherein the conclusion of the results of this study is given accompanied with some recommendations for further research.

2. Theory

In this chapter the relevant theory for this research is explained. Firstly, the ultrasonic waveguide is discussed. After this, the rheology of different fluids is explained. A closer look is taken at the velocity profiles and shear-rate of these fluids. Lastly, attention is paid to dimension analysis, which is used in this research to find an relation for the shear-rate without knowing the exact velocity profile of the fluid.

2.1. Ultrasonic waveguide

To measure the flow of a fluid, different viscometers can be used. A viscometer is an instrument to measure the viscosity of a fluid. For some fluids the viscosity needs to be determined for different shear-stresses. This is because not all fluids react linearly to the shear-stress. This will be explained further in the next section. The type of viscometer used depends on the fluid under invesigation. The fluid to be measured in this case is the molten salt, the fuel in the MSFR. Due to the extreme conditions inside the reactor not every viscometer is suitable. The molten salt has a high temperature of approximately $750\ C$, is radioactive and highly corrosive [2]. On top of this, previous research stated that the viscosity of the fuel salt is around 10 $mPa\ \ s$[9][10], a very low value which requires sensitive measuring methods. Research done by Rook [4] proposed the ultrasonic waveguide to measure the rheology of the molten salt. The figure below shows a schematic representation of an ultrasonic waveguide.

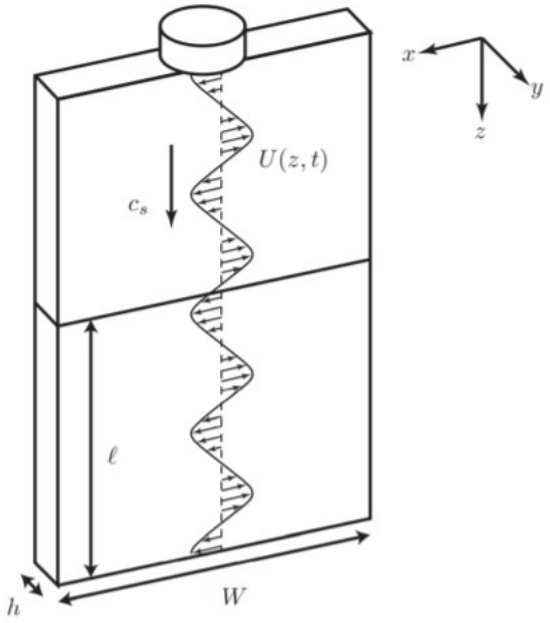

Figure 2: Schematic representation of the ultrasonic waveguide. W is the width, h the thickness and l is the length immersed in the fluid. The cilindrical part on top of the waveguide is the transducer, producing a shear-wave travelling with an amplitude $U(z,t)$ and a wave velocity c_s.[7]

The ultrasonic waveguide is only partially immersed in the molten salt when the rheology is measured. The advantage to this is that the piezoelectric transducer does not make contact with

the salt. This way the transducer stays under the temperature where it loses its piezoelectric effect.

2.1.1. Shear waves

The waves in the waveguide are polarised in the x-direction, as shown in figure 2. These type of waves are called shear waves, a type of transversal waves. Their polarisation is perpendicular to the propagation direction of the wave. The shear waves travel with velocity c_s and have an amplitude of $U(z,t)$.
It might be hard to imagine how the wave moves in the plate, as the plate is made of solid material. Actually, these are the molecules of the plate vibrating in the x-direction. The neighbouring molecules in the z-direction take on this same vibration with a wave velocity, c_s. The vibrating of the molecules in the plate move the adjacent fluid. The attenuation of the amplitude in the z-direction is completely determined by the shear-stress with this fluid. This is because the plate is very thin meaning no energy loss at the end of the plate and the frequency of the shear wave gives a non-dispersive wave which is explained in the next section. This way the attenuation of the amplitude is linked to the fluid's viscosity.

2.1.2. Frequency

To be sure the shear wave is only polarised in the x-direction only certain frequencies can be used for the experiment. Otherwise, higher modes can result the shear wave to move in the y-direction too. The range of possible frequencies is researched by Cegla [11] and also depends on the thickness h of the plate. The range of the frequency thickness where only the ground mode (SH0) is possible to exist is shown in figure 3.
The section with a frequency thickness of 0-1.5 $[MHz \;\; mm]$ shows that for shear waves only the ground mode is possible to exist. On top of this it shows that the phase velocity dispersion is constant. This means the wave is non-dispersive, i.e. the shape of the wave is constant over the propagation path. Thus, the attenuation of the amplitude is only due to the viscosity of the measured fluid.

2.2. Rheology of fluids

Rheology is the study of flow and deformation of materials. As the fuel of the MSFR is molten salt, a fluid, this research focuses mainly on the rheology of fluids. When a certain amount of stress is applied to any fluid this results in a deformation. The form of this deformation is dependent on the fluid itself. The relation between the velocity gradient and the shear-stress is fluid specific. Different fluids follow different rheology models. Two of the most common rheology models are described below.

2.2.1. Newtonian fluids

Newtonian fluids like water and air follow the most simple distribution. For these fluids the shear-stress applied to the fluid is linearly proportional to the shear-rate, the rate of deformation of the fluid. In a formula the shear-stress in one direction looks like:

$$\tau_{yx,Newton} = \quad \mu \;\; \frac{dv_x}{dy} \tag{1}$$

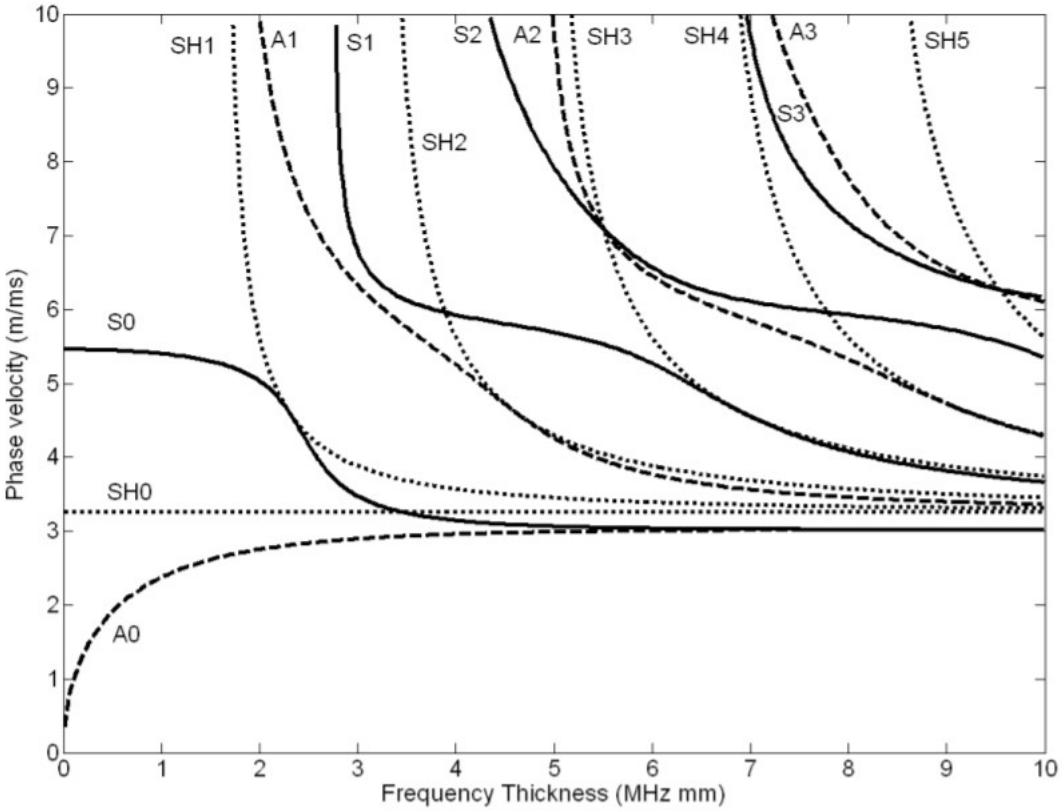

Figure 3: Phase velocity dispersion for a steel plate as a function of the frequency thickness. Shear wavemodes ( ), compressional wavemodes ( ), flexural modes ( ). [11]

This formula is called Newton's law of viscosity, described in [12]. The subscript yx means that the direction in which the shear-stress is pointed is in the x-direction and it has an effect on the fluid in the y-direction. The $\tau_{yx,Newton}$ is the shear-stress, μ is the dynamic viscosity and v_x is the velocity in the x-direction. The shear-rate is the change in the velocity profile in the direction perpendicular to the velocity. This shear-rate (in one direction) can also be described by $\dot{\gamma}$:

$$\dot{\gamma} = \frac{dv_x}{dy} \tag{2}$$

2.2.2. Power law fluids

Most fluids do not follow Newton's law of viscosity. Fluids that follow the Ostwald - de Waele model for the relation between the shear-stress and the deformation are known as Power law fluids. The Ostwald-de Waele model has a lot in common with Newton's law, as is shown below.

$$\tau_{xy} = \quad \mu_{app}(\dot{\gamma}) \quad \dot{\gamma} \tag{3}$$

The only thing that is different is the dependency of $\dot{\gamma}$ of the dynamic viscosity. This dynamic viscosity for power law fluids, μ_{app}, is called the apparent viscosity coefficient.

$$\mu_{app} = K \quad j\dot{\gamma}j^{n \ 1} \tag{4}$$

The K and the n in this formula are fluid specific. The fluid constant K is the consistency index and n is the flow index. From this apparent viscosity it is clear why these fluids are called 'power law' fluids. The name follows from the power n of $\dot{\gamma}$ in the relation.
Because of the power of the shear-rate these fluids behave a bit odd. When the flow index of a fluid, n, is bigger than 1, the deformation of the fluid becomes smaller once a bigger force is applied. These types of fluids are called 'shear thickening' fluids. The fluid seems to thicken as a bigger force is applied. When the flow index, n, is smaller than 1, the deformation of the fluid is increasing when the shear-stress increases. These fluids are called 'shear thinning', as they seem to become thinner once the shear-stress increases.
The behaviour of Newtonian fluids, shear thinning fluids and shear thickening fluids against the shear-stress is summarised in the following image.

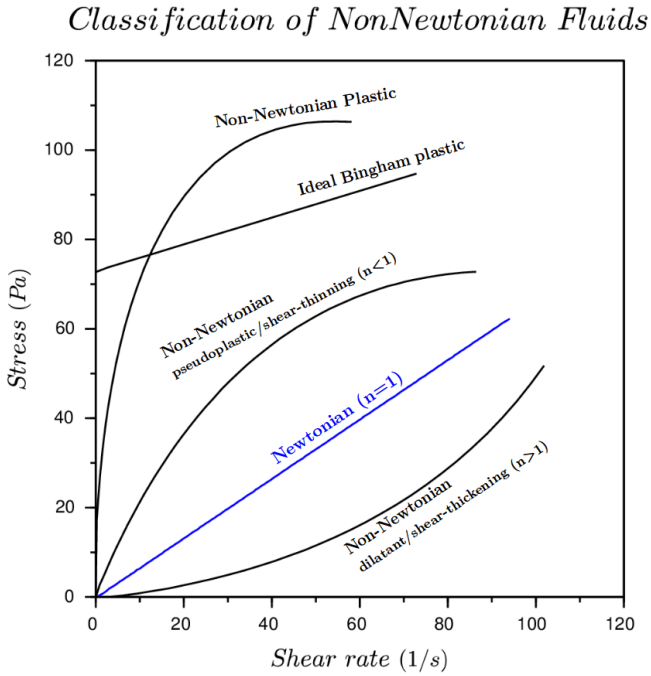

Figure 4: Plot of the shear-rate, $\dot{\gamma}$ [1/s] against the shear stress, τ [Pa] for Newtonian, shear-thinning $(n < 1)$ and shear-thickening $(n > 1)$ fluids.[13]

2.3. Energy equation for Newtonian fluids

The energy lost by the shear friction at $y = 0$, the boundary of the fluid with the waveguide, is given by the following formula, proposed by Rohde [7]:

$$\Delta P_\tau(z,t) = \quad 2 \quad \tau_0(z,t) \quad V_x(z,t) \quad W \quad dz \tag{5}$$

$\Delta P_\tau[W]$ is the energy loss at the surface of the waveguide. The -2 is because there is a loss of energy and it counts for both sides of the waveguide. $W[m]$, the width and $dz[m]$, the heigth describe the friction surface. This is multiplied by the shear stress $\tau_0[Pa]$ and the velocity of the shear-wave in the x-direction $V_x[m/s]$. The velocity for the shear-wave in the x-direction is known as this one is produced by the transducer. V_x at $y = 0$ is given as:

$$V_{x,y=0}(z,t) = B(z) \quad cos(kz \quad \omega t). \tag{6}$$

The unknown parameter is τ_0 as this depends on the fluid. The energy loss is related to the attenuation of the shear-wave in the waveguide. How this is related is explained in detail by Borstlap, [5] and Schuringa, [6].

The shear-stress, τ_0, for Newtonian fluids is given in the previous section by equation 1. The velocity profile is known analytically for Newtonian fluids as part of Stokes second problem [14]. The solution to Stokes second problem for the velocity is:

$$v_x(y,t) = A \quad exp(\quad \frac{y}{\delta_N} \quad cos(\omega t \quad \frac{y}{\delta_N})), \tag{7}$$

where $A[m]$ is the initial amplitude of the wave and $\delta_N = \sqrt{\frac{2\mu_0}{\rho_f \omega}}[m]$ is the viscous skin depth. The μ_0 and ρ_f in the viscous skin depth are the viscosity and the density of the fluid respectively. When this velocity is inserted in equation 1 and then this equation is on his turn filled in in equation 5, the viscosity can be determined from the attenuation of the shear-wave.

2.4. Energy equation for power law fluids

The determination of the rheological parameters from the attenuation is a bit harder for power law fluids. The equation for the energy loss is the same as for the Newtonian fluids like shown in equation 5. Relating the energy loss to the attenuation is also done in the same way as for Newtonian fluids. The energy balance can now be solved for the unknown shear stress τ_0. The difficulty for power law fluids comes in when trying to obtain the consistency index K and the flow index n. The equation of τ_0 for power law fluids, equation 3, is formed by the unknown fluid parameters, but also by the unknown shear-rate. The shear-rate cannot be determined by taking the derivative of the velocity profile as the velocity profile for non-Newtonian fluids cannot be determined analytically from Stokes second problem. The shear-rate should be determined in another way. Schuringa, [6] and Borstlap, [5], approached this shear-rate based on results of Ai and Vafai [8]. This research tries to find a solution for the shear-rate by executing a dimension analysis.

2.5. Dimension analysis

Dimension analysis is a way to relate different quantities that affect a process or motion. A difficult process, dependent on many parameters, is reduced to a smaller amount of dimensionless groups. This reduction of parameters makes a difficult problem easier to solve. The difficulty of dimension analysis is that one needs to have physical insight about the causal relationship between different quantities.
When executing a dimension analysis the first step is to decide on which independent physical variables the investigated quantity relies. In the case of this study the physical quantity under investigation is the shear-rate at the boundary $y = 0$, $\dot{\gamma}_0$. The variables on which this quantity depends are the following:

$$\dot{\gamma}_0 = f(B, \rho_f, \omega, K, n) \tag{8}$$

Here $\rho_f[kg/m^3]$ is the fluid density, $\omega[1/s]$ is the angular frequency, $K[kg/(m \quad s^2 \quad ^n)]$ is the consistency index and $n[\quad]$ is the flow index of the fluid. The reasoning behind the dependency on these variables is that the shear-rate is partially dependent on the fluid properties of the fluid in motion, ρ_f, K, n, and partially dependent on the motion of the waveguide characterised by

the variables ω and B. The dependency of the height, z is not taken into account directly, but the value for B depends on the height z. B is the velocity amplitude. The formula for B is:

$$B = \quad A(z) \quad \omega \tag{9}$$

Note that the magnitude of B depends on ω and $A(z)$ being the amplitude of $U(z,t) = A(z)$ $cos(kz \quad \omega t)$ in figure 2. Thus, the magnitude of B is not an entirely independent variable. After deciding on which variables $\dot{\gamma}_0$ depends, the equation is solved for all dimensions. How this is done exactly is shown in the appendix. The resulting equation from the dimension analysis is then:

$$\dot{\gamma}_0 = k \quad \omega \quad (\frac{B^2 \quad \rho_f}{\omega^n \quad K_m})^\delta \tag{10}$$

When 9 and 10 are combined this gives.

$$\dot{\gamma}_0 = k \quad \omega \quad (\frac{jBj \quad A \quad \rho_f}{\omega^n \quad ^1 \quad K_m})^\delta \tag{11}$$

In the part in parentheses some sort of Reynolds number can be recognised. In the numerator B, the amplitude velocity describes a velocity term, A describes a distance and ρ_f the density of the fluid. In the denominator, the term $\omega^n \quad ^1 \quad K_m$ can be seen as some sort of dynamic viscosity, μ_{app}, where $\dot{\gamma}_0$ is replaced by ω. This can be done as ω has the same dimensions as $\dot{\gamma}_0$, namely [1/s]. These observations lead to:

$$Re_{\dot{\gamma}_0} = \frac{B^2 \quad \rho_f}{\omega^n \quad K_m} \tag{12}$$

When equation 11 and equation 12 are combined, this gives us the final equation.

$$\frac{\dot{\gamma}_0}{\omega} = k \quad (Re_{\dot{\gamma}_0})^\delta \tag{13}$$

3. Experimental method

The main goal of this study is to find a relation for the shear-rate at $y = 0$, $\dot{\gamma}_0$, in the setup showed in figure 2. In the previous chapter the dimension analysis was explained and showed a relation for the shear-rate dependent of k, δ and Re_ω. The purpose of the experiments is to find the values of k and δ by varying Re_ω. This chapter will provide a complete description of the methods used to obtain the results in chapter 4.

Firstly, the computational simulation model of the waveguide immersed in a fluid will be described. This model is used to mimic the experimental setup with the ultrasonic waveguide and the motions of the fluid around it. Some aspects needed to write the code, like discretization, boundary conditions and constants, are also mentioned in this part.

Secondly, the code that differentiates B to obtain the corresponding values of $\dot{\gamma}_0$ is described. These values of the shear-rate for each value of B will be used to plot $\dot{\gamma}_0$ divided by ω over Re_ω from formula 12. From this plot the data will be fitted to find the values of k and δ as in equation 13.

The last section will describe the code for the differentiation of the other variable in Re that is independent of the fluid properties, ω. The rate obtained from this will also be plotted and fitted to find the values of k and δ.

3.1. Simulation code

The code that simulates the ultrasonic wave in the waveguide and the motion it creates in the fluid, is based on the code used by Borstlap [5] and Schuringa [6]. The scheme of Borstlap [5] for the code, which shows how the shear-rate is used and produced, is included in the appendix as figure 15.

In their research the code produces the values of $B(z)$, the attenuation for every height z. In order to get values for this attenuation the velocity profile and shear-rate are simulated for a boundary velocity $V_{x,y=0} = A \quad cos(\omega \quad t)$, where A is 1. This velocity is independent of z and B, where the boundary velocity produced by the waveguide is not, see equation 6. In this research only the first part of their code is used to calculate the shear-rate for different values of B and different angular frequencies ω. In the following sections the code is explained further.

3.2. Discrete differentiation

To determine the shear-rate, the derivative of the velocity profile is taken. However, to differentiate on a computer one cannot differentiate in the analytical way, i.e. over a infinitesimal small piece. Therefore, the computational approach of differentiating uses discretization. Discretization is the process of transforming a continuous function into a finite set of points. In this research discretization is done for constant intervals, h, as it makes the coding a lot easier. When taking the derivative of a discretized formula the slope of two points divided by the space in between them is taken. There are different ways to do this; some examples are forward difference, backward difference and central difference, shown in the figure below. Figure 5 shows

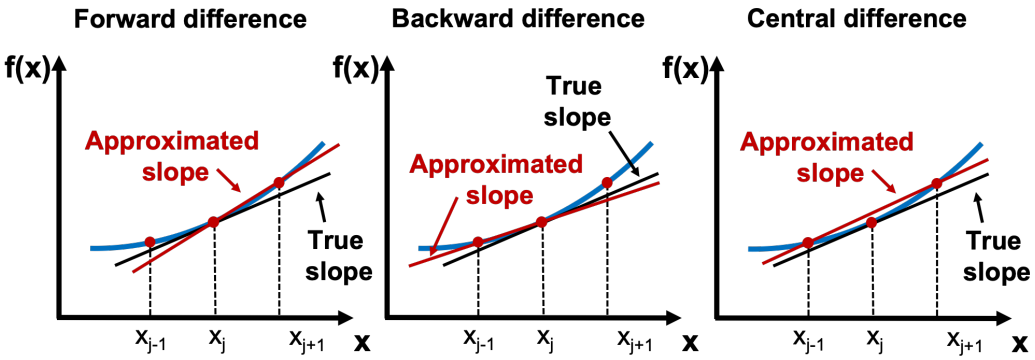

Figure 5: Approximation of the slope of a function $f(x)$ using different finite differentiation methods.[15]

that the central difference method gives the best approximation of the true slope.

This study is interested in the shear-rate at $y = 0$, a point on the boundary. Therefore, the central difference method cannot be used. This brings us to using the forward difference method, measuring the slope between the point at $y = 0$ and $y = 0 + h$.
The formula for calculating the forward difference is [16]:

$$f^0(x) = \frac{f(x+h) \quad f(x)}{h} \tag{14}$$

The order of the truncation error follows from the Taylor expansions and is in this case $O(h)$. $O(h)$ means in the order of h. To make the error smaller, with truncation error $O(h^2)$, the second order forward difference approach is used. How this formula is derived can be found in the appendix but the final formula is [17]:

$$f^0(x) = \frac{3f(x) + 4f(x+h) \quad f(x+2h)}{2h} \tag{15}$$

Equation 15 is then used in the code to calculate $\dot{\gamma}_0$ at different times by filling in V_x at $y = 0$, $y = h$ and $y = 2h$.

Discretization asks for discrete steps in time and space. These will be defined as:

$$t_i = i\Delta t, y_j = j\Delta y, z_k = k\Delta z, \tag{16}$$

with i, j and k positive integers. In a function dependent on t, y and z the step will be indicated with sub- and superscripts. For example:

$$a(y_j, z_k, ti) = a^i_{j,k} \tag{17}$$

The time index is written in the superposition and the place indices are written in subscript in alphabetical order. This discretization will be used when the looping is explained in more detail.

3.3. Boundary velocity and velocity profile

The velocity at $y = 0$ is the same as the velocity of the waveguide. This is a result of the so-called no slip condition. The velocity of the shear-wave in the waveguide is known. As shown in figure 2, the transducer produces a wave creating a deformation in the x-direction with magnitude $U(z,t)[m]$, given by:

$$U(z,t) = A(z) \quad sin(kz \quad \omega t). \tag{18}$$

$A(z)$ is the amplitude of the shear-wave $[m]$, k is the wavenumber $[m \ ^{1}]$, z is the location along the z-axis of the waveguide $[m]$, ω is the angular frequency $[s \ ^{1}]$ and t is the time $[s]$.
Deriving equation 18 over time and remembering the formula for the velocity amplitude, $B(z)[m/s]$ (equation 9), gives:

$$\frac{\partial U(z,t)}{\partial t} = V_x(z,t)\mathbf{j}_{y=0} = B(z) \quad cos(kz \quad \omega t). \tag{19}$$

Although B in formula 19 is a function of z, it is not dependent on z in this calculation of the shear-rate, $\dot{\gamma}_0$. In the real experiment B follows from the height z as the shear wave in the waveguide is damped more when the z is higher, i.e. deeper in the fluid. In this calculation B is just a number determining the amplitude of the shear-wave at $y = 0$ and thus not dependent on z. It is easier to loop directly over B instead of looping over z as looping over z makes the cosinus function complicated. The boundary velocity in the code is simplified to the following:

$$V_x(t)\mathbf{j}_{y=0} = B \quad cos(\omega t). \tag{20}$$

This velocity is independent of z. But why is it permitted to simplify the cosine to a function independent of z? Note that kz inside the cosine results in a shift of the cosine.

$$V_x(t)\mathbf{j}_{y=0} = B \quad cos(kz \quad \omega t) \tag{21}$$

When z is bigger, the cosine starts a bit more to the right and with a smaller z the cosine starts more to the left. This shift adds again at the end because t is determined by ω in a way that the same amount of periods of the shear wave is produced. The final calculated shear-rate is the time average of the total absolute shear-rate. How this is done is described in the section about time averaging. Because the time average is taken, the periodical behaviour does not matter anymore in the final answer. Therefore leaving out the shift caused by z in the cosine also does not matter. This leaves us with the simplified boundary velocity from equation 20.

The velocity profile in the fluid is created by looping forward in time, central in space (FTCS). The simplified Navier-Stokes equation, earlier calculated by Borstlap,[5] is rewritten into a discrete form, looking like this:

$$v_{j,k}^{i+1} = v_{j,k}^{i} \quad \frac{1}{\rho_f}\frac{\Delta t}{2\Delta y} \quad (\tau_{j+1,k}^{i} \quad \tau_{j \ 1,k}^{i}) \tag{22}$$

In this equation, i, j and k are the time and space indices as described above in 16.

3.4. Input variables

To determine k and δ from equation 13, $\dot{\gamma}_0/\omega$ is calculated for different values of Re_{γ_0}. Re_{γ_0} depends on B, ω and fluid parameters. As the fluid parameters cannot be changed individually, B and ω are changed. The shear-rate is calculated for these different values of B and ω.
The values that are put into the code are summarised in tables in this section. This section contains the values that are the same for looping over B and looping over ω. The values that are different when B is changed from when ω is changed are summarised in sections 3.5 and 3.6 respectively.

3.4.1. Constants

In the next table an overview of the quantities of the steel waveguide used in the experiments by Rook [4] is given. The same values are used in our simulation model to mimic the experiment as accurately as possible.

Quantity	$h[m]$	$L[m]$	$c_s[m/s]$	$\rho_s[kg/m^3]$
Value	0.202e-3	2.035e-1	3.083e3	7.876e3

Table 1: Waveguide properties from the experimental setup of Rook[4]. L and h are the total length of the waveguide and the thickness respectively, c_s is the velocity of the shearwave and ρ_s is the density of the material the waveguide is made of, stainless steel.

The other constants concern the fluid that is measured. The fluid properties of the different shear-thinning fluids used in the simulations are displayed in the next table.

Fluid	Consistency index $K[Pa \quad s^n \quad ^1]$	Power index $n[\quad]$	Density $\rho_f[kg/m^3]$
Ketchup	6.47	0.300	1136
Soybean oil	2.18	0.510	930
Human blood	9.267e-3	0.828	1060

Table 2: Fluid properties for different shear-thinning fluids. The values for ketchup are retrieved from [18], for soybean oil the used source is [19], the rheological properties K and n of blood were found in [20] and the density of blood is from [21].

3.4.2. Boundary and initial conditions

As explained earlier, at the boundary where $y = 0$, the velocity is the same as the velocity in the waveguide, see equation 6. This cosine function is the boundary condition of the left boundary at all times.
The boundary condition for the velocity far away from the waveguide, at $y \; ! \; 1$, approaches 0 at all times t. This is because it is far from the moving surface and the velocity is damped out by the fluid.
The last condition that is set is the initial condition for the velocity. As the waveguide starts moving at $t = 0$, the fluid is assumed to stand still for all y for $t < 0$. These 3 conditions are displayed together in the table below.

$V_x(0,t) = Bcos(\omega t)$	$y = 0, 8t$
$V_x(y,t)$! 0	y ! 1 , $8t$
$V_x(y,t) = 0$	$8y, t < 0$

Table 3: Table presenting the boundary and initial conditions of the velocity together with the values of y and t they apply to.

3.4.3. Step sizes

Because everything is discretized and equal spatial steps are preferred the amount of steps needs to be set.
First, the amount of steps in the z-direction is $N_z = 1000$. In table 1, $z = 2.035e \quad 1[m]$, so $\Delta z = 2.035e \quad 4$.
In the y-direction the right boundary is set as far as possible, so that the boundary condition $v_x = 0$ is approached. Schuringa determined this value for soybean oil with:

$$y_{end} = 50 \quad \sqrt{\frac{2 \quad K \quad \omega^n \quad 1}{\omega \quad \rho_f}}. \tag{23}$$

For ketchup Schuringa had a smaller value for this but for practical reasons the calculation for y_{end} is taken to be the same for every fluid. As y_{end} was the biggest for soybean oil according to Schuringa, this formula is taken for all fluids to be sure the boundary condition is approached. Note that y_{end} depends on ω so y_{end} and the step size Δy will vary when ω is altered. It also depends on the fluid properties so every fluid has a different Δy and y_{end}. The space in the y-direction is divided into $N_y = 500$ steps. The spacing in the y-direction, Δy, is defined as:

$$\Delta y = \frac{y_{end}}{N_y} = 0.1 \quad \sqrt{\frac{2 \quad K \quad \omega^n \quad 1}{\omega \quad \rho_f}}. \tag{24}$$

The values of Δy are calculated using the fluid properties from table 2 and equation 24, and are listed in the following table.

Fluid	Δy
Blood	20.2e-9
Ketchup	5.85e-9
Soybean oil	22.2e-9

Table 4: Values of Δy for different fluids.

The last discretized parameter is the time, t. Eight periods are simulated so that an equilibrium can set in and the results can be measured as accurately as possible for the least simulations [6]. The final time, T is then determined by ω like:

$$T = \frac{8 \quad 2\pi}{\omega}. \tag{25}$$

The time is divided into $N_t = 24000$ equal steps. As the time depends om ω the final time, T and the spacing Δt also depend on ω:

$$\Delta t = \frac{T}{N_t} = \frac{2\pi}{3 \quad \omega} \quad 10 \quad ^3. \tag{26}$$

3.4.4. Time average

Because the shear-rate is a periodical function, the time average is taken. It takes some time for the shear-rate to become a nice periodic function. This is because the fluid needs some time to adjust to the motion induced by the waveguide. We are only interested in the shear-rate after it has a constant oscillating behaviour. The location where the periodicity starts is the place where the shear-rate is 0 for the first time. From this part on the time derivative of $\dot{\gamma}_0$ is taken for the three fluids.
The time averaging is done by integrating along the time axis using the trapezoidal rule. This calculates the absolute sum of the shear-rate. This sum then needs to be divided by the total time T minus the time needed to adjust, t_{equi}, to get the time averaged shear-rate, as shown in equation 27.

$$< \dot{\gamma}_0 >= \frac{1}{T \quad t_{equi}} \int_{t_{equi}}^{T} \frac{3V_x(0) + 4V_x(\Delta y) \quad V_x(2\Delta y)}{2\Delta y} \tag{27}$$

3.5. Varying B to change $Re_{\dot{\gamma}_0}$

In order to get the shear-rate for different values of $Re_{\dot{\gamma}_0}$, the process of calculating the shear-rate has to be repeated for different values of B. This is done by setting a loop for B around the original code that generates $\dot{\gamma}_0$. The loop varies the value of B in the boundary velocity from equation 6. The different values of B are 10 equally spaced values between $B = 10^5[m/s]$ and $B = 10^6[m/s]$. Remember B being a function with A and ω, as in equation 9. When varying B, the amplitude A generated by the waveguide is varied. The values of B are 10 evenly spaced values between 10^5 and 10^6. These values are chosen because the results for B from Borstlap [5] and Schuringa [6] lie in this range. The value of ω has to remain constant here because Re_ω also depends on ω.

$$\omega = 2\pi \quad 3.7 \quad 10^6 \tag{28}$$

Only one parameter a time is altered to see the effect of only that parameter on the shear-rate. The figure below shows the flow-diagram used for the loop over B.
As no other parameters, like the time and the y-coordinate, depend on B the looping is done only over the part that calculates the velocity and the shear-rate. In the next section will be explained that, when ω is varied, the time range changes too.

3.6. Varying ω to change $Re_{\dot{\gamma}_0}$

The other parameter $Re_{\dot{\gamma}_0}$ depends on which is independent of the fluid properties is ω. To check whether the shear-rate has the same dependency when ω is changed, the code is looped over ω too. The differnt values used for ω are equally spaced between $\omega = 2pi \quad 5 \quad 10^5[s \quad ^1]$ and $\omega = 2pi \quad 10^7[s \quad ^1]$. Looping over ω is a bit more complicated. For every ω a distinct time range has to be calculated as the final time depends on ω, according to equation 25. In this part of the code B is kept constant at $B = 10^5$. Because the shear wave is now oscillating at an other frequency this affects on the boundary velocity. So in addition to the time range, the boundary velocity from equation 6 is changed for every ω, resulting in a different value for the shear-rate. The remaining part of the code is approximately the same as the code for B, but because the time range changes for every value of ω the time averaging of the rate is also done inside the loop. The flow diagram of this code with the differences to the code for B is showed below.

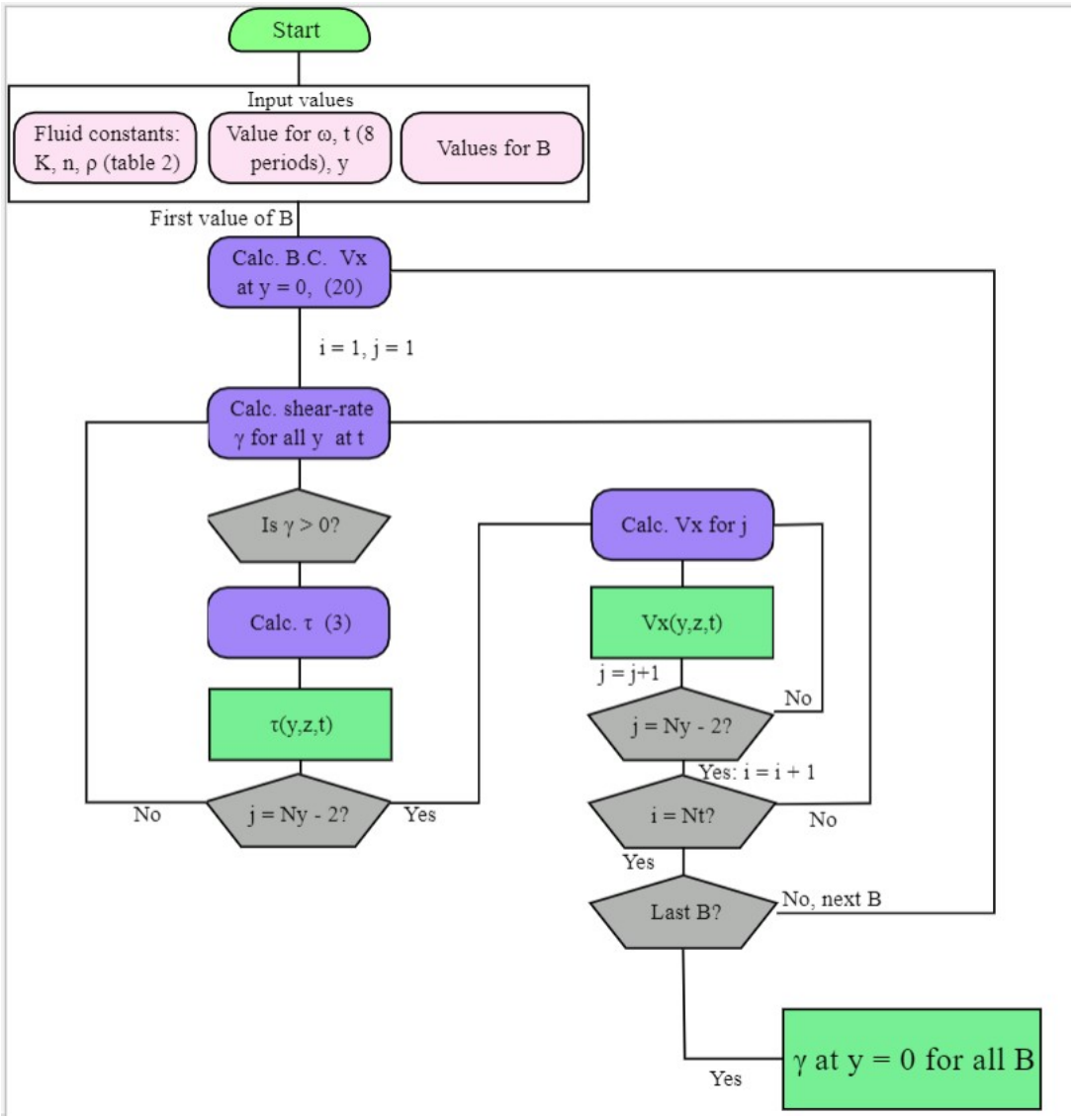

Figure 6: Flow diagram for varying B, with the shear-rate at the left boundary for all B as outcome.

3.7. Data processing: Fitting k and δ

To fit the constants k and δ, the shear-rate obtained by variation of ω and B is firstly divided by ω, to match the left side of equation 13. The left side of this equation is plotted on the y-axis versus $Re_{\dot{\gamma}_0}(B)$ and $Re_{\dot{\gamma}_0}(\omega)$, depending on whether B or ω is varied. After this, the values of k and δ can be determined, applying least squares fitting. The code tries to fit the data on the x-axis and the data on the y-axis to the formula $y = k \ \ x^{\delta}$. The results are displayed in the next chapter.

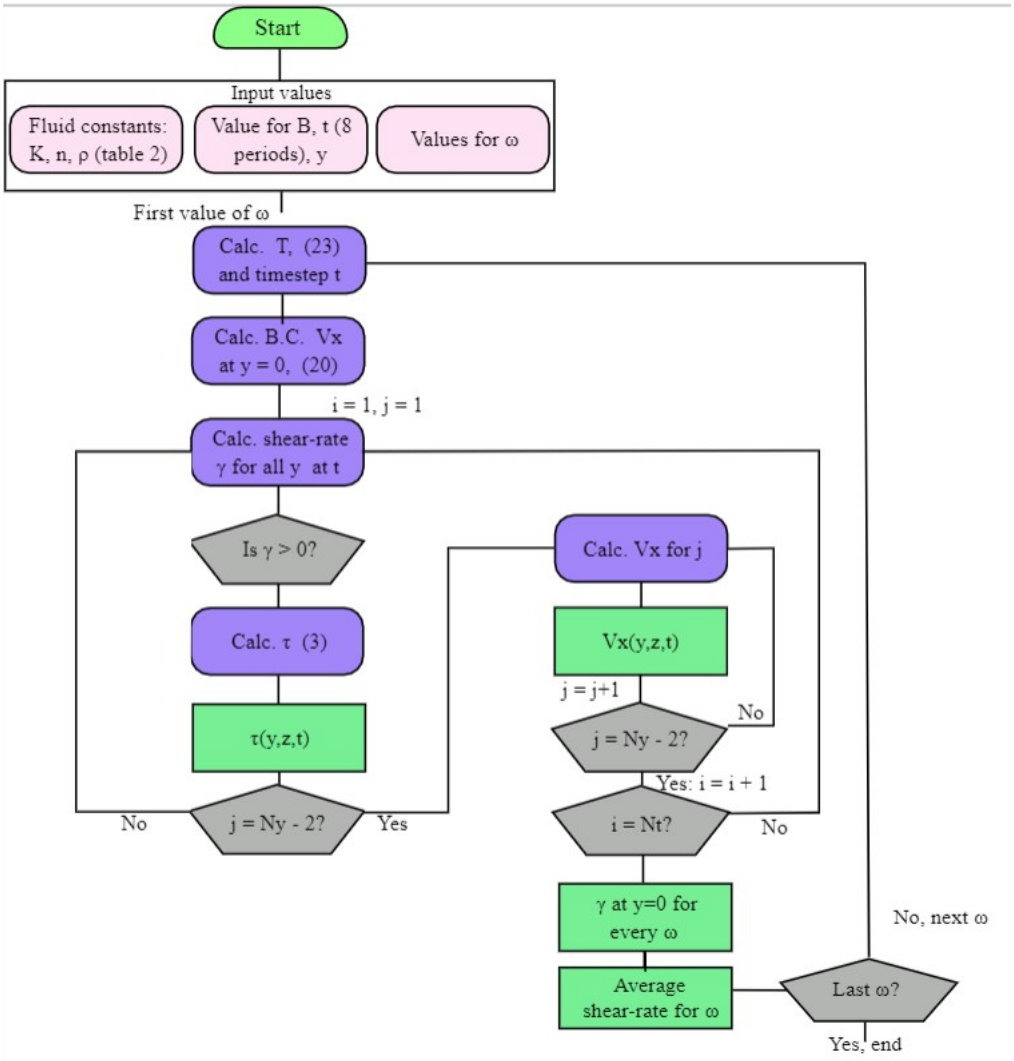

Figure 7: Flow diagram for varying ω, with the shear-rate at the left boundary and the time averaged shear-rate for all ω as outcome.

4. Results and discussion

This chapter presents the results obtained from computational simulation. The results are explained and discussed where they differ from expected values. The first section presents the fits for k and δ for different fluids when B in $Re_{\dot{\gamma}_0}$ is varied. In the second section presents the results for when ω in $Re_{\dot{\gamma}_0}$ is varied.

4.1. Results for different values of B

This section shows the results for the shear-rate when B is altered. The value for ω is constant at $\omega = 2\pi \quad 3.7 \quad 10^6[s \ ^1]$.

4.1.1. Shear-rate over time

The shear-rate at $y = 0$, $\dot{\gamma}_0$, is plotted over time. The plots are presented below for the fluids: blood, ketchup and soybean oil from left to right. The value of B for which the rate is plotted is $B = 10^5[m/s]$.

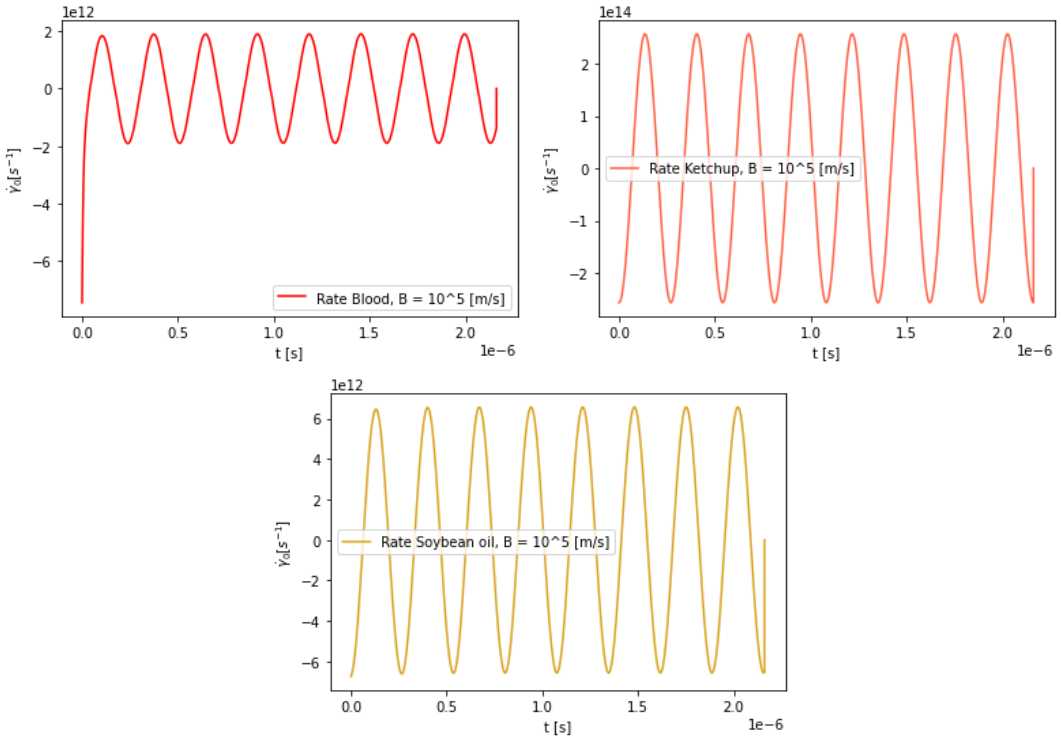

Figure 8: Plot of the shear rate over time for blood, ketchup and soybean oil from left to right. $B = 10^5[m/s], \omega = 2\pi \quad 3.7 \quad 10^6[s \ ^1]$.

The shear-rate at starts at a value dependent on the boundary velocity and the value of Δy. This is because of the way the shear-rate is calculated, with equation 15: because the velocity at all y but $y = 0$ is still 0 at that time step it results in $\frac{3}{2}\frac{B}{y}[s \ ^1]$. The value of B is the same for the three fluids but equation 24 states that the value of Δy is fluid dependent. The starting values of the shear-rate differ per fluid due to this dependency.

After some time the fluid is in a constant oscillatory motion resulting in a constant oscillatory behaviour of the shear-rate. Compared to the starting value the maximal amplitude for blood becomes much smaller when the maximal amplitude for ketchup and soybean oil stays approximately the same.

4.1.2. Time averaged shear-rate

The time averaged shear-rate of the three fluids is discussed in this section. As mentioned above the time average is only taken from the point where the shear-rate is zero for the first time. The averaged rate is plotted here for the three different shear-thinning fluids.

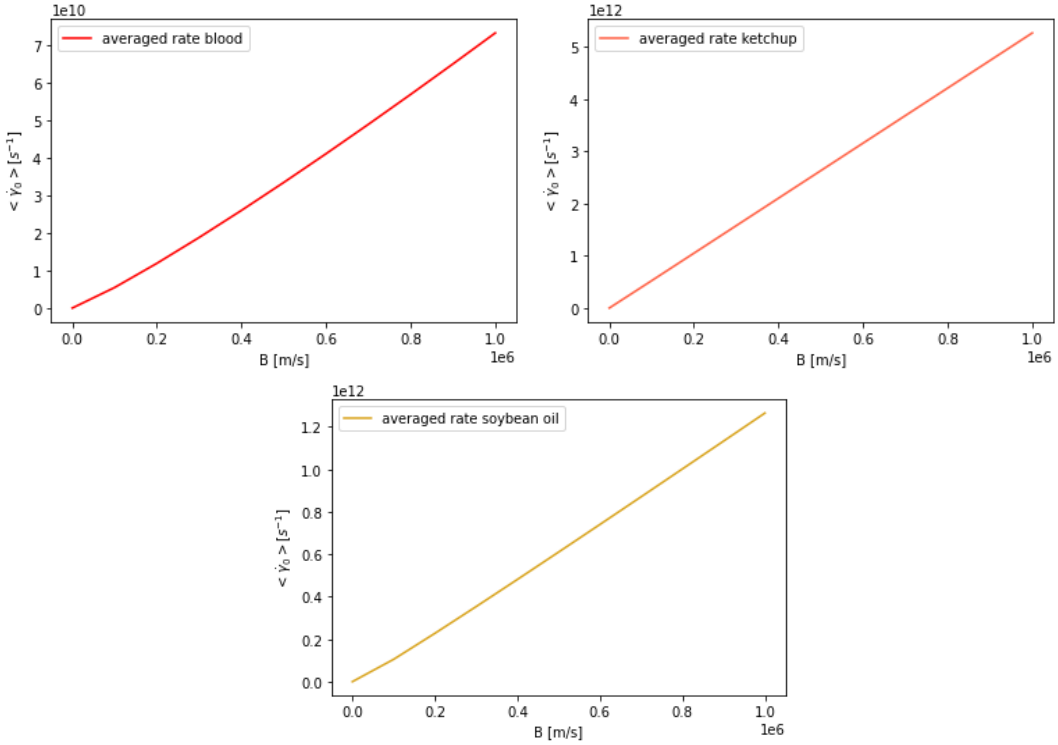

Figure 9: Plot of the time averaged shear-rate $[1/s]$ for different values of $B[m/s]$. From left to right: blood, ketchup, soybean oil.

The $< \dot{\gamma}_0 >$ at $y = 0$ is almost linear for all three fluids. The shear-rate increases when the value for B increases, which is logical. For blood the values of $< \dot{\gamma}_0 >$ are much lower than for the other two fluids. This follows logically from the smaller amplitude in figure 8. When the time average is taken it is shown that the shear-rate for soybean oil is lower than the shear-rate for ketchup, and the shear-rate for blood is the lowest. This is expected because soybean oil is less shear-thinning than ketchup, i.e. it has a higher flow index n, and blood has the highest flow index.

4.1.3. Plotting $\dot{\gamma}_0/\omega$ as a function of $Re_{\dot{\gamma}_0}(B)$

In order to fit the constants k and δ from equation 13, $\dot{\gamma}_0$ is divided by ω and plotted as a function of $Re_{\dot{\gamma}_0}(B)$.

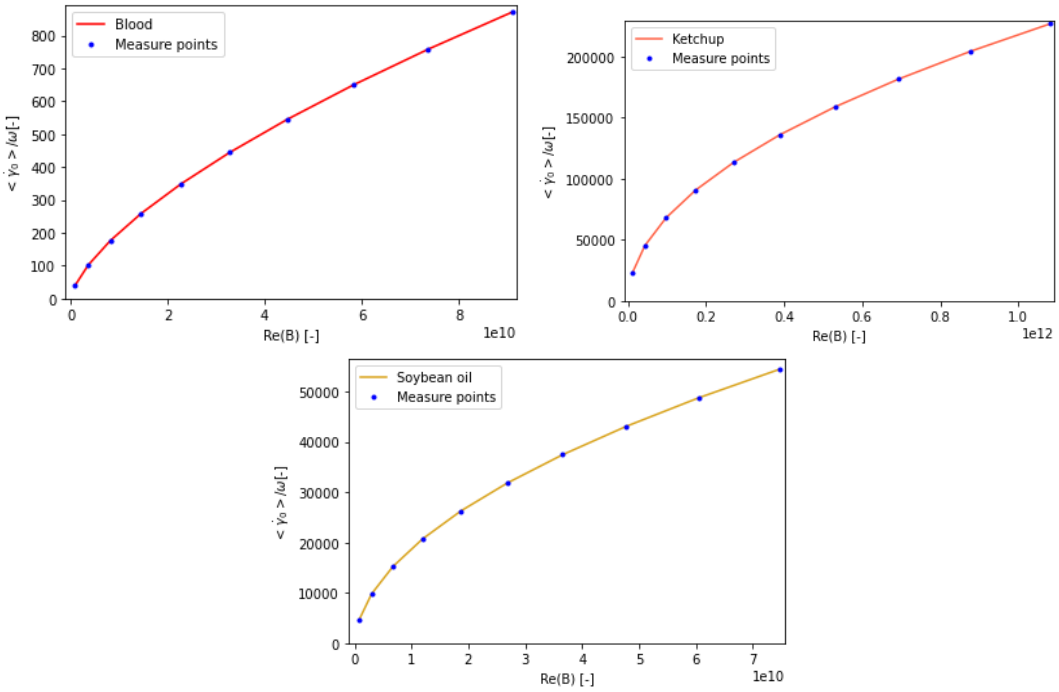

Figure 10: Plot of the shear-rate at $y = 0$ divided by ω over $Re_\omega(B)$. From left to right: blood, ketchup, soybean oil.

To the naked eye the shape of these plots looks the same. The values of B for calculating $Re_{\dot{\gamma}_0}$ where equally spaced and the same for the three fluids, but because $Re_{\dot{\gamma}_0}$ is also dependent on the fluid properties. Now, the measure points are not equally spaced anymore and lie on different values of $Re_{\dot{\gamma}_0}$ for the different fluids. This can be seen in the different range of the x-axis for the different fluids. The measure points for which B the shear-rate is calculated are plotted as blue dots. In order to find out how much alike the plots really are, the constants k and δ are fitted through each of these curves.

4.1.4. Fitted parameters k and δ

The values for k and δ for each fluid are fitted and presented in the table below.

Fluid	**Fitted** k	**Fitted** δ
Blood	5e-05	0.66
Ketchup	0.212	0.50
Soybean oil	0.095	0.53

Table 5: Fitted values of k and δ for different fluids.

The k and δ for ketchup and soybean oil are in the same range, but not completely the same. On the other hand the values for blood, especially the fitted k, are in a different range. If the relation for the shear-rate in equation 13 had been correct, the fitted k and δ had to be the same for the three different fluids.

Because we have the fitted parameters, the line for different fluids can be plotted over the same $Re_{\dot{\gamma}_0}$. This is done and shown below.

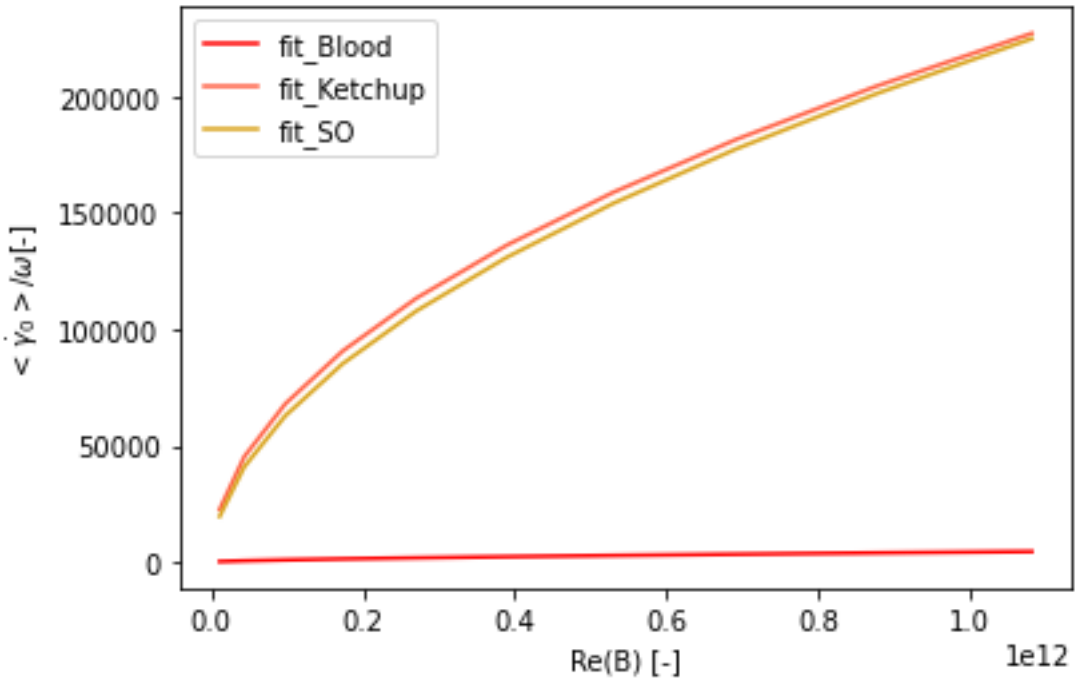

Figure 11: Fitted lines for the three different fluids plotted over Re_ω.

In the fit the values for blood are relatively low compared to the values for ketchup and soybean oil. The values of ketchup and soybean oil are similar. Even though the shapes looked the same, in figure 10 we can see that blood differs a lot in amplitude. An explanation for this difference could be that there is another, fluid dependent, dimensionless parameter. Another dimension analysis for this dimensionless parameter should be done and researched to find the correct equation for $\dot{\gamma}_0$. Because the values for ketchup and soybean oil are close to each other it is likely that this dimensionless parameter depends on the consistency index K_m, as this K_m is almost the same for ketchup and soybean oil but is a lot smaller for blood.

4.2. Results for different values of ω

In this section the results are shown for the shear-rate when ω is altered. The value for B in this section is $10^5[m/s]$, equal to the first value in the loop over B and chosen because it is a value in the range of values for B for the set up obtained by Schuringa [6].

4.2.1. Time averaged shear-rate

The value for $\dot{\gamma}_0$ averaged over time is plotted in this section for every ω. Similar to the time

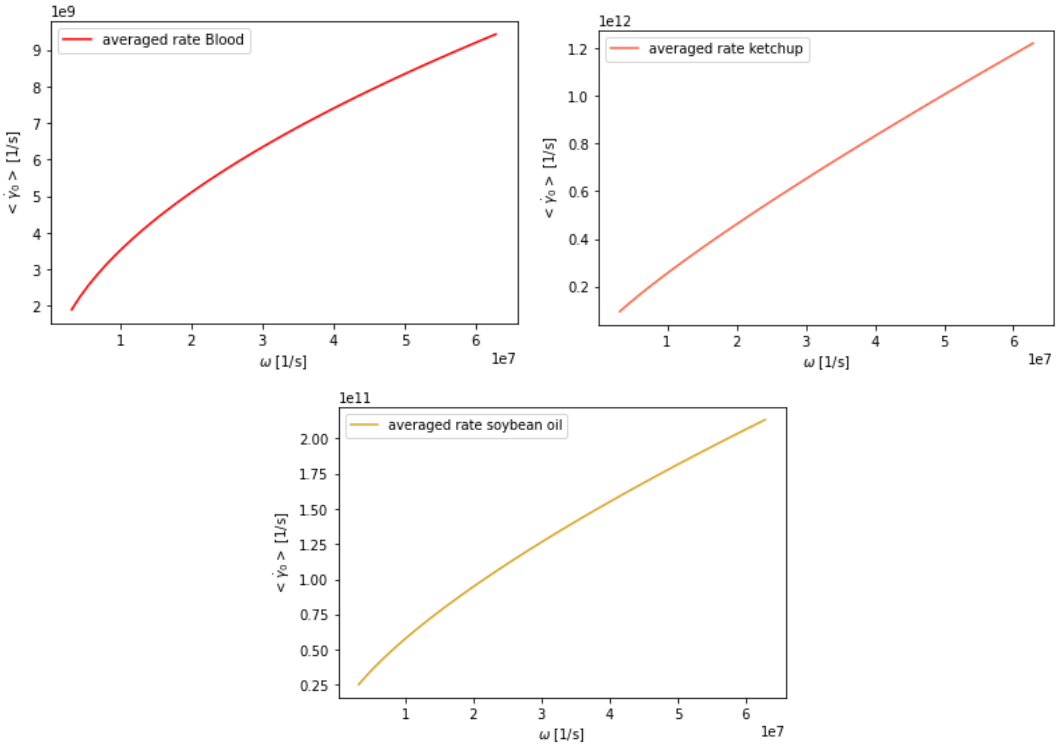

Figure 12: Time averaged shear-rate at $y = 0$ over ω. From left to right: blood, ketchup, soybean oil.

averaged shear-rate over B, the time averaged shear-rate increases almost linearly over ω. The values for $< \dot{\gamma}_0 >$ are the smallest for blood and the biggest for ketchup. This is as expected from the flow index n, which is the highest for blood and the lowest for ketchup.

4.2.2. Plotting $\dot{\gamma}/\omega$ as a function of $Re_{\dot{\gamma}_0}(\omega)$

To fit k and δ, a plot for $\dot{\gamma}_0/\omega$ as a function of $Re_{\dot{\gamma}_0}(\omega)$ is made. Because the Reynolds number depends exponentially on ω, with in the exponent a fluid specific parameter, n, the range of the x-axis differs a lot for each fluid. Therefore, they are firstly presented separately and, after fitting, plotted in the same figure.

In figure 13 the measure points are plotted as blue dots. The values of ω were equally spaced, but the density of measure points is larger in the region with low $Re_{\dot{\gamma}_0}$. This is another result of the exponential dependency of $Re_{\dot{\gamma}_0}$ on ω. The shape of the plots look the same for each fluid,

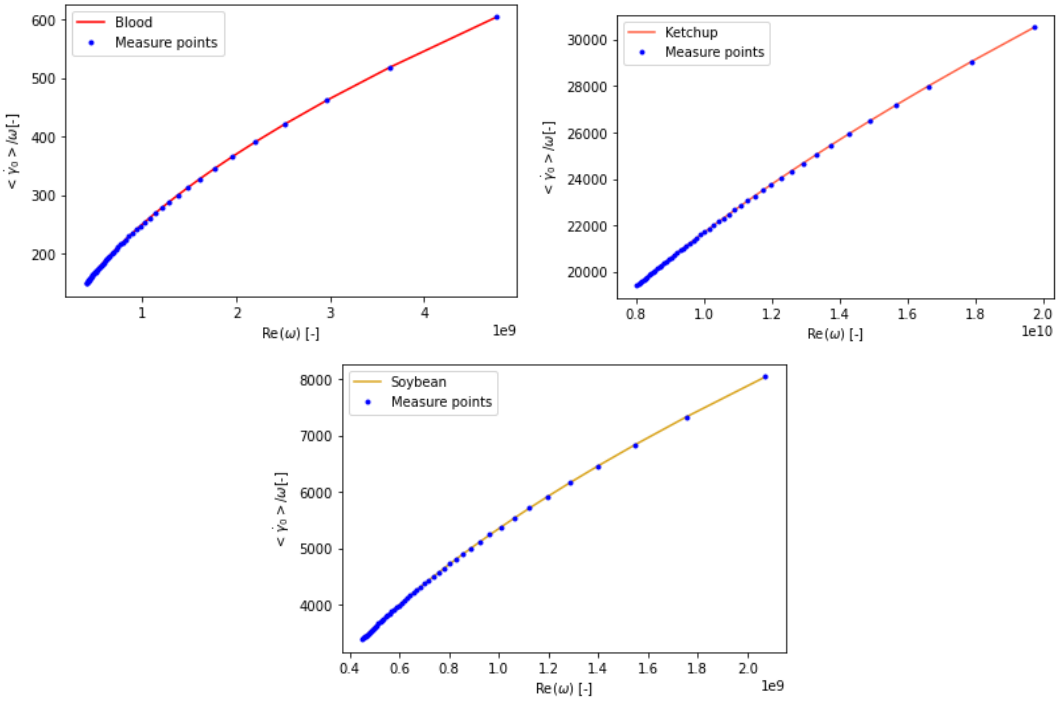

Figure 13: Plot of the shear-rate at $y = 0$ divided by ω over $Re_\omega(\omega)$. From left to right: blood, ketchup, soybean oil.

more curved for lower values of $Re_{\dot{\gamma}_0}$ and gradually becoming flatter. To compare them better the values are fitted and plotted over the same $Re_{\dot{\gamma}_0}$ in the next section.

4.2.3. Fitted constants k and δ

When fitting through the measure points we must keep in mind that the fit can differ from the actual values because there are fewer measure points for higher $Re_{\dot{\gamma}_0}$. This brings a uncertainty that can be solved by increasing the amount of measure points or by distributing ω differently such that it gives more measure points for higher $Re_{\dot{\gamma}_0}$. The fitted values from figure 13 are presented in table 6.

Fluid	**Fitted** k	**Fitted** δ
Ketchup	0.203	0.50
Blood	0.002	0.56
Soybean oil	0.045	0.56

Table 6: Values for k and δ for blood and soybean oil obtained by fitting the graph form figure 13 to the formula $y = k \quad x^\delta$.

The values for δ are in the same range for the three fluids. The values of k are further from each other. This is an indication for an extra dimensionless parameter. The fitted k is the largest for ketchup and the smallest for blood. The extra dimensionless parameter is still likely to be dependent on the consistency index, K_m as this follows the same gradation, i.e. smallest for blood and largest for ketchup.
The graphs with the fitted constants are plotted below over the same $Re_{\dot{\gamma}_0}$.

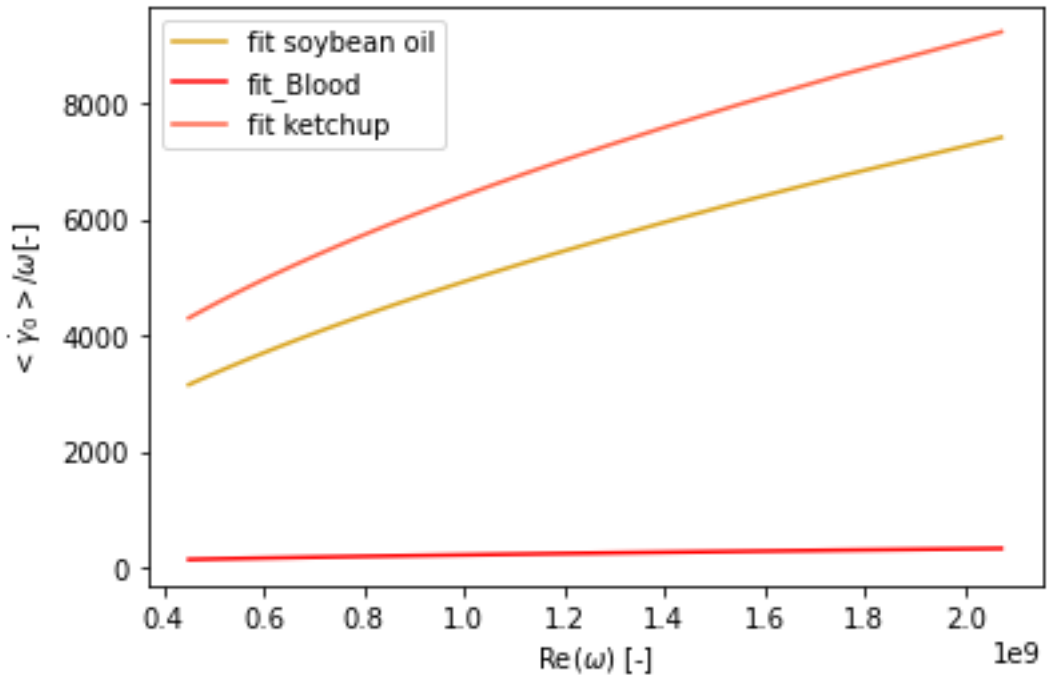

Figure 14: Fitted lines for the two different fluids plotted over Re_ω.

In the fit the effect of the different values of k is clearly visible. The curves of the lines are similar, due to the similar δ, but the height of the lines differs due to different values for k. If the formula from the dimension analysis was proven to be right these lines should have been the same for each fluid. They should also have followed the same relation as the graphs in figure 11. As they do not follow this same relation the conclusion would be that there is a second dimensionless parameter involved in the relation for the shear rate at $y = 0$. This second dimensionless parameter is likely dependent on the consistency index $K_m[kg/(m\ \ s^2\ \ ^n)]$. This parameter was already taken into account in the first dimension analysis, so one or more other parameters that were not taken into account should be added as well.

5. Conclusion and recommendations

The aim of this research was to find a relation for the shear-rate of shear-thinning fluids in the ultrasonic waveguide setup. In order to find this relation a dimension analysis was executed. To check whether the obtained relation was correct and to find the unknown pre-factor, k and the unknown power, δ to the dimensionless parameter, the computer simulation of the setup was performed. This simulation showed the dependency of the shear-rate on the angular velocity, $\omega[s^{-1}]$ and the velocity amplitude, $B[m/s]$. The shear-rate from the simulation was then plotted against the dimensionless parameter. With least squares fitting of this data, the dimensionless parameters k and δ were found.

The relation for the shear-rate of shear-thinning fluids in the ultrasonic waveguide setup is not found yet. However, the dependency of the shear-rate to B and ω was calculated and plotted.

On top of this, there were clear agreements for the fitted k and δ between ketchup and soybean oil when B was varied. For blood the fitted k and δ were different. The reason for this can be another dimensionless parameter that was missed in the dimension analysis.

When ω was varied the fitted δ was in the same range for the three different fluids. The fitted k differed significantly between the three fluids. The value of k was the smallest for blood and the biggest for ketchup, this the same for the consistency indices for these fluids, i.e. blood has a low K_m where ketchup has the highest K_m. This can indicate for a missing dimensionless parameter dependent on K_m.

The overall conclusion of this research is that the found relation for the shear-rate misses a dimensionless parameter that probably depends on the consistency index $K_m[kg/(m\ \ s^{2-n})]$. If this is the case the dimensionless parameter should also depend on a parameter that was not taken into account in the executed dimension analysis. This parameter could be for example the height on the waveguide, $z[m]$, the viscous skin depth of power law fluids, $\delta_{PL}[m]$, or the pressure of the fluid at $z + dz$ on the fluid at z with unit $[kg/(ms^2)]$. These parameters have good units to form a dimensionless parameter in combination with K_m.

Further research can be done about the 'missing' dimensionless parameter depending on the parameters discussed.

When the shear-rate is found this can be applied to calculate the rheological properties of shear-thinning more accurately in the ultrasonic waveguide setup. To be able to find the rheological properties of other fluid types, their shear-rate should be investigated too.

References

[1] GEN IV International Forum. Generation iv goals, 2021. "[Online] Available at: https://www.gen-4.org/gif/jcms/c-9502/generation-iv-goals [Accessed 4-November-2021]".

[2] SAMOSAFER. The concept of the molten salt fast reactor, 2021. "[Online] Available at: https://samosafer.eu/project/concept/ [Accessed 4-November-2021]".

[3] Martin Rohde. Molten salts, 2021. "[Online] Available at: https://www.martinrohde.nl/topics.html [Accessed 4-November-2021]".

[4] Remco Rook. *Viscosity determination of newtonian fluids using shear ultrasonic guided wave attenuation*. Master's thesis, TU Delft, March 2020.

[5] Lotte Borstlap. *Numerical study on the determination of the rheological properties of power-law fluids in the ultrasonic waveguide experiment*. Bachelor's thesis, TU Delft, August 2020.

[6] Olivier Schuringa. *Determination of rheological properties of Power-law fluids using a numerical ultrasonic waveguide viscometer*. Master's thesis, TU Delft, July 2021.

[7] M. Rohde, R. Rook, and S. Mastromarino. Determining the rheology of power law fluids with a waveguide at high-frequency shear waves, September 2021.

[8] L. Ai and K. Vafai. An investigation of stokes' second problem for non-newtonian fluids. *Numerical Heat Transfer, Part A: Applications*, 47:955–980, 6 2005.

[9] R. Serrano-López, J. Fradera, and S. Cuesta-López. Molten salts database for energy applications. *Chemical Engineering and Processing: Process Intensification*, 73:87–102, 2013.

[10] Stanley Cantor. Density and viscosity of several molten fluoride mixtures, March 1973.

[11] F.B. Cegla. *Ultrasonic waveguide sensors for fluid characterisation and remote sensing*. PhD thesis, Imperial College London, January 2006.

[12] H.E.A. Van den Akker and R.F. Mudde. *Fysische transportverschijnselen*. Delft Academic Press, fourth edition, 2014.

[13] Simscale Documentation. Non-newtonian models, 2021.

[14] Chi-Min Liu. Complete solutions to extended stokes' problems. *Mathematical Problems in Engineering*, 9 2008.

[15] Q. Kong. *Python Programming And Numerical Methods: A Guide For Engineers And Scientists*. Academic Press, first edition, 2020.

[16] Desmond J. Higham. *An Introduction to Financial Option Valuation*. Cambridge Academic Press, ninth edition, 2013.

[17] C. Vuik, F.J. Vermolen, M.B. van Gijzen, and M.J. Vuik. *Numerical methods for ordinary differential equations*. Delft Academic Press, VSSD, second edition, 2018.

[18] Vojtěch Kumbár, Sylvie Ondrušíková, and Šárka Nedomová. Rheological properties of tomato ketchup. *Potravinarstvo Slovak Journal of Food Sciences*, 13:730–734, 09 2019.

[19] Nelson Moraga, Alejandra Torres, ABEL GUARDA, and Maria Galotto. Non-newtonian canned liquid food, unsteady fluid mechanics and heat transfer prediction for pasteurization and sterilization. *Journal of Food Process Engineering*, 34, 12 2011.

[20] Sangho Kim, Young I. Cho, Abraham H. Jeon, Bill Hogenauer, and Kenneth R. Kensey. A new method for blood viscosity measurement. *Journal of Non-Newtonian Fluid Mechanics*, 94:47–56, 11 2000.

[21] John Cutnell and Kenneth Johnson. *Physics*. Wiley, fourth edition, 1998.

Appendix

5.1. Full derivation of the dimension analysis

The dimension analysis is started with determining the fysical variables. The quantity under investigation is written as a function of these fysical variables.

$$\dot{\gamma}_0 = f(B, \rho_f, \omega, K, n) \tag{29}$$

Now this function is written as a constant times the variables to a power. Like this:

$$\dot{\gamma}_0 = k \quad (B)^{\alpha} \quad (\rho_f)^{\beta} \quad (\omega)^{\delta} \quad (K)^{\epsilon} \quad (n)^{\zeta} \tag{30}$$

The units of these variables are compared as follows:

$$[s \quad ^{1}] = [\quad] \quad ([m/s])^{\alpha} \quad ([kg/m^{3}])^{\beta} \quad ([s \quad ^{1}])^{\delta} \quad ([\frac{kg}{m \quad s^{2} \quad n}])^{\epsilon} \quad ([\quad])^{\zeta} \tag{31}$$

The following step is to make a balance for all the different units.

- s: -1 = -α - δ - (2-n) ϵ
- m: 0 = α -3 β - ϵ
- kg: 0 = β + ϵ

Solve these balances to obtain the correct values for the powers and fill these in in equation 30. This leads to the following equation:

$$\dot{\gamma}_0 = k \quad \omega \quad (\frac{B^{2} \quad \rho_f}{\omega^{n} \quad K_m})^{\delta} \tag{32}$$

This is the final equation. The data from the simulations will be fitted to obtain the correct values for k and δ.

5.2. Code used by Borstlap and Schuringa

Below the scheme Borstlap [5] and Schuringa [6] used to get values of $B(z)$ is presented. They used $B(z)$ to calculate the consistency and flow index, K and n, of different fluids. As this research focuses on the shear-rate, $\dot{\gamma}$, only the red boxed part is used.

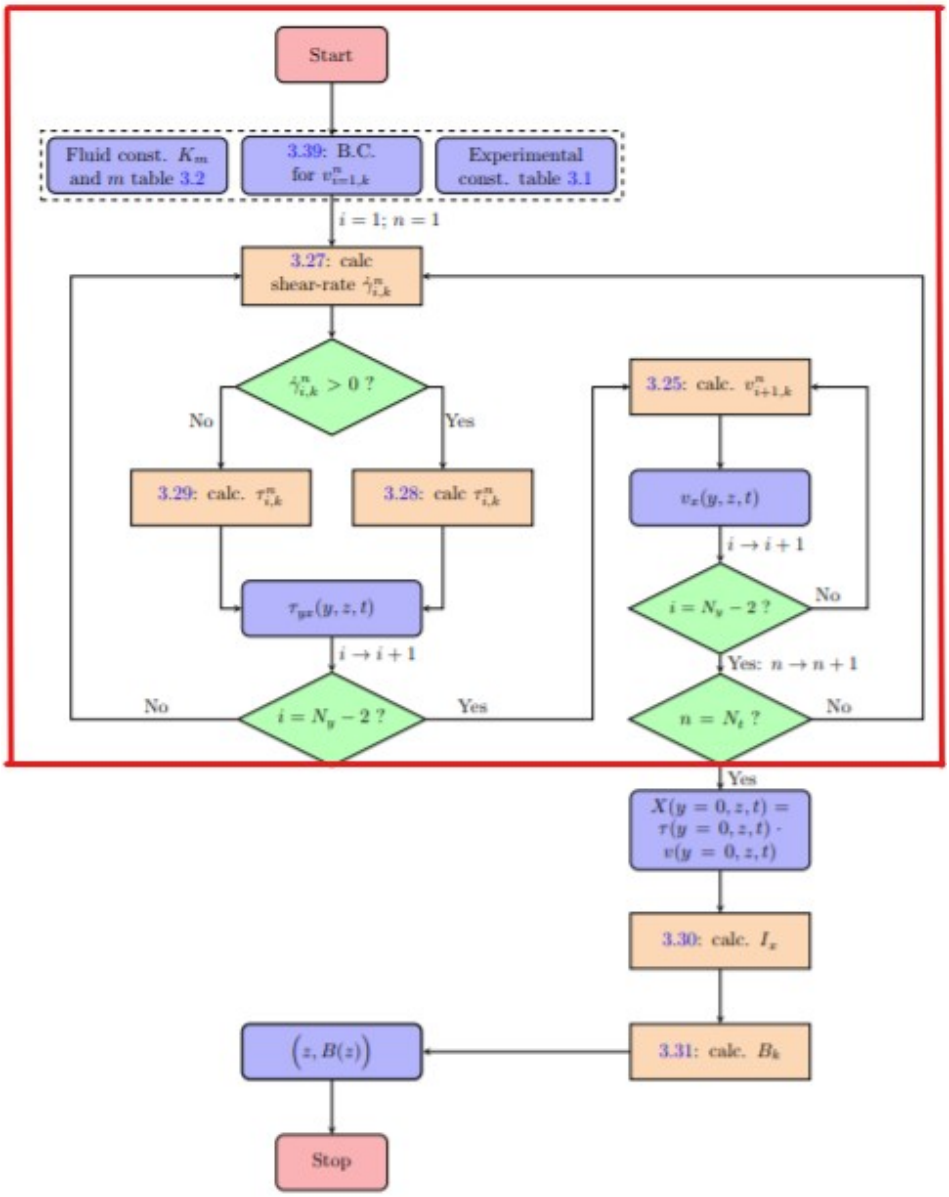

Figure 15: Flow diagram of the code used by Borstlap to simulate the ultrasonic waveguide setup producing values for $B(z)$ [5]. The part in the red box is used in this research to produce values for the shear-rate at y = 0.

5.3. Derivation second order forward difference formula

The derivative of the velocity profile has to be determined at the left boundary of the interval where $y = 0$. The asked truncation order is $O(h^2)$. To solve this 3 points need to be taken, x, $x + h$ and $x + 2h$ making:

$$f^0(x) = \frac{af(x) + bf(x + h) + cf(x + 2h)}{h} \tag{33}$$

The Taylor expansions are given by:

- f(x) = f(x),
- f(x+h) = f(x) + hf'(x) + $\frac{h^2}{2}$ f"(x) + h.o.t.,
- f(x+2h) = f(x) + 2hf'(x) + $2h^2$ f"(x) + h.o.t..

They must follow 3 conditions:

1. f(x): $\frac{a}{h}$ + $\frac{b}{h}$ + $\frac{c}{h}$ = 0,
2. f'(x): b + 2c = 1,
3. f"(x): h$\frac{b}{2}$ + 2hc = 0.

Solving these conditions for a, b and c gives $a = \quad 3/2$, $b = 2$ and $c = \quad 1/2$. Leading to our final equation:

$$f^0(x) = \frac{3f(x) + 4f(x + h) \quad f(x + 2h)}{2h} \tag{34}$$